Article ID: 1000-7032(2026)02-0314-07

Impact of Well Thickness on Static and Dynamic Behavior of InGaN Light-emitting Diode with Single Quantum Well

CHEN Guichu[1*], HE Longfei[2], PENG Kun[3]

(1. *Department of Electronic Information, Zhaoqing University, Zhaoqing* 526061, *China*;
2. *Institute of Semiconductor, Guangdong Academy of Sciences, Guangzhou* 510650, *China*;
3. *School of Microelectronics, Fudan University, Shanghai* 200433, *China*)

* *Corresponding Author, E-mail: gchenbox@163. com*

Abstract: In this paper, we present a circuit model of single-quantum-well InGaN/GaN light-emitting diodes based on the standard rate equations. Two rate equations describe carrier transport processes occurring in separate confinement heterostructure and quantum well respectively, and the third equation describes the varied photons in quantum well. By using the presented model, impacts of quantum well thickness on the static and dynamic performances are investigated. Simulated results show that LED with 4 nm well exhibits better light-current (*L-I*) performance, but LED with 3 nm well presents wider 3 dB modulation bandwidth. It reveals that high carrier density in quantum well is detrimental to the static performance, but beneficial to the dynamic performance.

Keywords: single quantum well; rate equations; circuit model; *L-I* performance; modulation bandwidth

CLC number: TN312. 8 **Document code**: A

DOI: 10. 37188/CJL. 20250235 **CSTR**: 32170. 14. CJL. 20250235

量子阱厚度对 InGaN 单量子阱发光二极管静态和动态特性的影响

陈贵楚[1*], 贺龙飞[2], 彭 坤[3]

(1. 肇庆学院 电子信息系, 广东 肇庆 526061;
2. 广东省科学院 半导体研究所, 广东 广州 510650;
3. 复旦大学 微电子学院, 上海 200433)

摘要: 在标准速率方程基础上提出了 InGaN/GaN 单量子阱发光二极管的电路模型,该模型通过两个速率方程分别描述载流子在隔离限制异质结与量子阱中的输运过程,第三个速率方程则描述量子阱中光子的动态特征。利用所建模型,我们系统研究了量子阱厚度对器件的静态与动态特性的影响。模拟结果表明,4 nm 量子阱宽的 LED 展现出更优异的光功率-电流特性,而 3 nm 量子阱宽的 LED 则具有更宽的 3 dB 调制带宽,这同时揭示出量子阱中的高载流子密度虽不利于静态性能,却能有效提升动态性能。

关 键 词: 单量子阱; 速率方程; 电路模型; 光功率-电流特性; 调制带宽

收稿日期: 2025-11-05; **修订日期**: 2025-11-24
基金项目: 广东省自然科学基金面上项目(2025A1515011593)
Surpported by Guangdong Basic and Applied Basic Research Foundation(2025A1515011593)

1 Introduction

High-speed InGaN/GaN light-emitting diodes (LEDs) are of recent interest for visible-light communication (VLC) in future light-fidelity (Li-Fi) networks[1]. As a complement to traditional radio frequency (RF) technology, VLC systems can achieve multi-Gb/s data rates by modulating LEDs[2-3], which function as illumination and communication sources simultaneously. In addition to Li-Fi networks, high-speed visible-emitting LEDs also have application in polymer optical fiber communication (POF)[4] and underwater wireless optical communication (UWOC)[5]. Because the bandwidth of conventional broad-area LEDs used for lighting is limited to tens of MHz, micro-LEDs have been developed to achieve the higher bandwidths needed for VLC applications[6-7].

A numerical analysis of the rate equations is a powerful tool for studying InGaN LEDs. Studying the behavior of carriers and photons has been used in some powerful simulation software such as SPICE. An essential process in the calculation of static and dynamic behavior by using this software is the solution of the differential rate equations. In previous studies, Chen and his co-worker derived an equivalent circuit model based on the two-level rate equations for the GaN-based LEDs, which proved that both n-type barrier doping and quantum well number have a significant effect on the modulation bandwidth[8-9]. Li and his team used an equivalent circuit model of InGaN micro-LEDs to investigate that the RC constant or carrier recombination rate was the main limiting factors of the bandwidth[10]. Rashidi used the small-signal rate equations to construct a small-signal equivalent circuit of InGaN LEDs, which proved that the LEDs with low RC time constant and short recombination lifetime exhibit high-speed behavior[11].

In this work, we present a circuit model based on solving rate equations for InGaN single quantum well (SQW) LEDs by using Spice software. In this model, only two levels are considered and hence there are three rate equations altogether: two for carreirs and one for photons. The static and dynamic properties of SQW LEDs are derived from the direct current (DC) and alternative current (AC) simulations of the circuit model, respectively. The simulated results show that quantum well thickness has a significant effect on the static and dynamic behavior of LEDs.

2 Device Structure and Transport Process

The active region of our structure is a 3 nm (4 nm) $In_{0.2}Ga_{0.8}N$ quantum well confined with two 100 nm separate confinement heterostructure (SCH) GaN layers. The schematic representation of the carrier transport processes occurring in the SQW LED is shown in Fig. 1. Carriers are injected from the cladding region into the SCH layer, and subsequently diffuse toward the QW layer under forwarding bias with a time delay of τ_d and are captured by the single QW with a capture rate of $1/\tau_c$. The total delay experienced by unconfined carriers in the SCH region (N_s) is defined as the SCH delay $\tau_s=\tau_d+\tau_c$. In our study, the radiative and non-radiative recombinations of carriers in the SCH region are neglected. After captured by QW, the carrier population in the QW (N_w) can be altered by two processes: recombination (radiative and non-radiative), with rate $1/\tau_r$, and thermionic emission (escape) to the SCH region, with rate $1/\tau_e$. The radiative and non-radiative recombinations include Shockley-Read-Hall (SRH), spontaneous radiative, and Auger recombinations. These recombinations are described by the *ABC* model[12], where *A*, *B*, and *C* are the recombination coefficienst related to three recombinations, respectively, *i. e.*, the decay rate of carriers in QW is expressed as

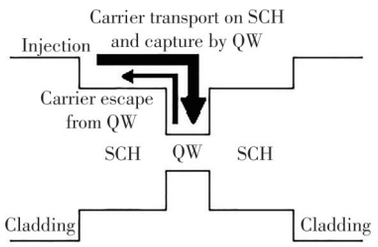

Fig.1　Schematic view of carrier transport processes in a SQW LED

$$\frac{N_w}{\tau_r} = AN_w + BN_w^2 + CN_w^3 . \quad (1)$$

3 Construction of Circuit Model

We consider two independent carrier rate equations for the left SCH and QW layer. To consider the effect of confinement on the well, the equations are normalized with respect to the SCH and well volumes respectively. By supposing the current injection from the left SCH to QW, two rate equations for the carriers in the SCH, quantum well, respectively, are[13]

$$\frac{dN_s}{dt} = \frac{I}{qV_{sch}} - \frac{N_s}{\tau_s} + \frac{N_w}{\tau_e}\frac{V_{qw}}{V_{sch}}, \quad (2)$$

$$\frac{dN_w}{dt} = \frac{N_s}{\tau_s}\frac{V_{sch}}{V_{qw}} - \frac{N_w}{\tau_e} - (AN_w + BN_w^2 + CN_w^3), \quad (3)$$

the above mentioned two rate equations of carriers are coupled with a photon rate equation

$$\frac{ds}{dt} = BN_w^2 - \frac{s}{\tau_p}, \quad (4)$$

where I is the injected current, q is the electronic charge, the meaning of N_s, N_w, τ_s, and τ_e has been mentioned above, s is the photon population, τ_p is the lifetime of photon, V_{sch} is the volume of the SCH layer, V_{qw} is the volume of quantum well. Due to the same area of the cross section (A_c) for the SCH and QW layer, $\frac{V_{qw}}{V_{sch}}$ is equal to $\frac{L_{qw}}{L_{sch}}$, in which L_{qw} and L_{sch} are the length of the SCH and QW layer.

We define the carrier population in the SCH and QW region using

$$N_s = N_{s0}\exp\left(\frac{qV_s}{\eta_s kT}\right), \quad (5)$$

$$N_w = N_{w0}\exp\left(\frac{qV_w}{\eta_w kT}\right), \quad (6)$$

where N_{s0} and N_{w0} are the equilibrium carrier numbers in the SCH and QW layer, respectively; while η_s and η_w are the corresponding diode ideality factor, typically set equal to 2. k is the Boltzmann constant. T is the absolute temperature. V_s and V_w are the voltages across the SCH and QW region, respectively.

In order to derive the equivalent circuit representation from Eq. (2)-(4), the standard circuit elements are brought to transform the rate equations into the specific type which suits the formation of circuit model. The differential term $qV_{sch}\frac{dN_s}{dt}$ in Eq. (2) is denoted as $C_s\frac{dV_s}{dt}$, with C_s expressed as

$$C_s = \frac{q^2V_{sch}N_{s0}}{2kT}\exp\left(\frac{qV_s}{2kT}\right), \quad (7)$$

and $qV_{qw}\frac{dN_w}{dt}$ in Eq. (3) is also denoted as $C_w\frac{dV_w}{dt}$, with C_w expressed as

$$C_w = \frac{q^2V_{qw}N_{w0}}{2kT}\exp\left(\frac{qV_w}{2kT}\right), \quad (8)$$

where C_s and C_w are a capacitance representing the charge storage effect in the SCH and QW region, respectively. However, the type of Eq. (4) is not effective to form corresponding circuit model, therefore, an improvement is adopted to satisfy this requirement. The optical output power P_{out} is represented by a nodal voltage[14], namely,

$$V_{out} = P_{out} = \frac{\eta_0 A_c hc^2}{6\lambda_s}s = \alpha s, \quad (9)$$

where η_0 is extracted light efficiency of LED, λ_s is the peak wavelength, h is the Planck's constant, c is the velocity of light. With this modification, Eq. (2)-(4) are transformed into the following type:

$$I = C_s\frac{dV_s}{dt} + I_s - I_w, \quad (10)$$

$$I_s - I_w = C_w\frac{dV_w}{dt} + aI_w + bI_w^2 + cI_w^3, \quad (11)$$

$$bI_w^2 = C_p\frac{dV_{out}}{dt} + \frac{V_{out}}{R_p}, \quad (12)$$

where I_s means the transport current in SCH layer, $I_s = \frac{qV_{sch}N_s}{\tau_s}$, and I_w means the escape current from QW layer, $I_w = \frac{qV_{qw}N_w}{\tau_e}$, $a = \frac{A\tau_e}{qV_{qw}}$, $b = \frac{B\tau_e^2}{q^2V_{qw}^2}$, $c = \frac{C\tau_e^3}{q^3V_{qw}^3}$, $R_p = \alpha\tau_p$, $C_p = \frac{1}{\alpha}$. The intrinsic circuit model based on Eq. (10)-(12) is formed in Fig. 2.

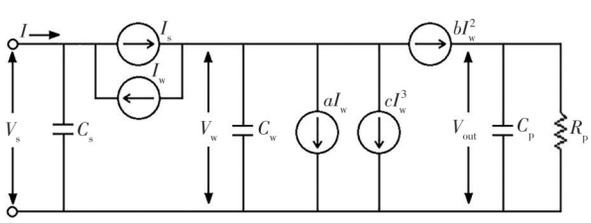

Fig. 2 The equivalent intrinsic circuit model of SQW LED

4 Determination of Model Parameters

The primary parameters of interest are the carrier transport time in the SCH region (τ_s), and the carrier escape time from the well to SCH layer (τ_e). The carrier transport time in the SCH (τ_s) is the sum of diffusion time (τ_d) in the SCH and the capture time (τ_c) in the well. We have just considered electrons as the carriers in our model, the diffusion time becomes[15-16]

$$\tau_d = \frac{L_{sch}^2}{2D_n}, \tag{13}$$

where D_n is the electron diffusion constant. The carrier capture time (τ_c) is the time duration of capturing carriers from the 3-dimensional (3D) states (SCH or the region above the well) to the 2-dimensional (2D) state (inside the well). The previous works revealed that the capture time (τ_c) linearly decreases with the increasing well thickness (L_{qw}) approximately[17-18]. On account of known values of τ_c for $In_{0.2}Ga_{0.8}N$ SQW and MQW structure[13], we deduce the relation between τ_c and L_{qw}:

$$\tau_c = 0.7 - 0.1875\frac{L_{qw}}{L_{qw0}}\,(\text{ps}), \tag{14}$$

where $L_{qw0} = 3$ nm.

The carrier escape time (τ_e) is the time of carriers escape from the well to the SCH layers and it is related to thermionic emission over the SCH layers. In fact, it is the time that carriers escape from the 2D state (inside the well) to the 3D state (SCH layers). If the carriers obey Boltzmann statistics, the escape time τ_e is expressed as[19]

$$\tau_e = \frac{2\pi m_e L_{qw}^2}{kT}\exp\left(\frac{E_B}{kT}\right), \tag{15}$$

where m_e is the effective electron mass, and E_B is the effective barrier height. E_B also represents the conduction band offset between $In_{0.2}Ga_{0.8}N$ and GaN material, and its calculation method is described in Ref. [19].

The values of all model parameters used in the Spice simulation have been collected in Tab. 1.

Tab.1　Model parameters used in the simulation[13-14,19]

Symbol	Description	Value	Unit
L_{qw}	QW thickness	3, 4	nm
L_{sch}	SCH layer thickness	100	nm
A_c	Area of cross section	30×30	μm^2
λ_S	Peak wavelength	420	nm
η_0	Extracted light efficiency	0.1	
c	Light velocity in the vacuum	3×10^8	$m\cdot s^{-1}$
q	Electron charge	1.6×10^{-19}	C
h	Planck's constant	6.62×10^{-34}	J·s
k	Boltzmann constant	1.38×10^{-23}	$J\cdot K^{-1}$
T	Temperature of active layer	300	K
D_n	Electron diffusion constant	39.41	$cm^2\cdot s^{-1}$
E_B	Effective barrier height	0.53	eV
m_0	Free electron mass	9.1×10^{-31}	kg
m_e	Effective electron mass	0.18	m_0
A	SRH recombination coefficient	5.4×10^7	s^{-1}
B	Radiative recombination coefficient	2×10^{-11}	$Cm^3\cdot s^{-1}$
C	Auger recombination coefficient	2×10^{-30}	$Cm^6\cdot s^{-1}$
τ_d	Diffusion time in SCH layer	1.269	ps
τ_{c1}	Capture time by SQW (L_{qw}=3 nm)	0.7	ps
τ_{c2}	Capture time by SQW (L_{qw}=4 nm)	0.45	ps
τ_{e1}	Escape time from SQW (L_{qw}=3 nm)	122.7	ps
τ_{e2}	Escape time from SQW (L_{qw}=4 nm)	281.1	ps
τ_p	Lifetime of photon	2.5	ps

5 Simulation Results and Discussion

The area of two types of LEDs considered here is micro-size (30 μm×30 μm), and the structure of both LED samples is identical except the quantum well thickness (L_{qw} is equal to 3 nm and 4 nm, respectively). Fig. 3 shows the light-current (*L-I*) curves of both LEDs, which derived from the DC Spice simulation of their circuit model. Both curves saturate, in other words, the efficiency droop appears when the injected current becomes greater, which is due to Auger recombination dominating the recombination process. The inferior *L-I* performance of LED with 3 nm well to one with 4 nm well is attributed to that the narrow quantum well has more carrier density within, leading to higher Auger recombination (CN_w^3 from Eq. (1)), which is harmful to the light output of LED. As reported earlier[20], the efficiency droop of InGaN LED is relieved along with increasing thickness of the active region, which also supports our simulation result.

It has been proved that when the device is in the micro scale, the modulation bandwidth is not limited by RC time but by recombination lifetime[21], therefore our simulation results are received for the case where parasitics are ignored. Fig. 4 shows the

frequency response of both LEDs at 18 mA and 30 mA bias current, which is derived from the AC simulation of Spice model. The LED with 3 nm well exhibits superior performance to one with 4 nm well, which is attributed to two reasons. Firstly, the modulation bandwidth at −3 dB, $f_{-3\,\mathrm{dB}}$ can be expressed as

$$f_{-3\,\mathrm{dB}} = \frac{1}{2\pi\tau_{\mathrm{r}}}, \tag{16}$$

τ_{r} is effective recombination lifetime which can be derived from Eq. (1) as follows

$$\tau_{\mathrm{r}} = \frac{1}{A + BN + CN^2}. \tag{17}$$

The LED designed with narrow SQW facilitates more carriers density and higher recombination rate and thus higher optical modulation bandwidth.

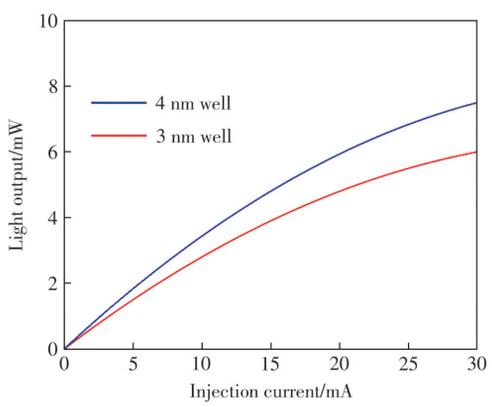

Fig.3 Light output *vs* injection current for both LEDs

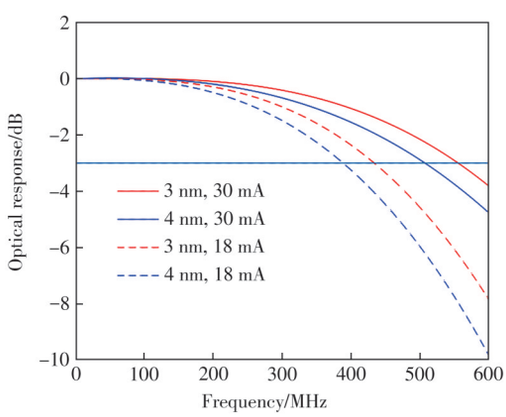

Fig.4 Modulation response of both LEDs at two bias currents

Secondly, the carrier population in QW is replenished by the SCH delay at rate $1/\tau_{\mathrm{s}}$, at once being depleted by the escape at rate $1/\tau_{\mathrm{e}}$. Because τ_{e} is far greater than τ_{s}, the depletion of carrier at escape rate is almost ignored. As is shown in Fig. 3, the narrow-well LED exhibits wider modulation bandwidth than the wide one (556 *vs* 508 MHz at 30 mA), which accords approximately with the experimental results published by Ref. [22]. According to Eq. (16), the carrier recombination lifetime (τ_{r}) of both LEDs is expected to be 0.28 ns and 0.31 ns, respectively. Obviously, the modulation performance is mainly determined by the slowest time parameter. Although the SCH delay time τ_{s} of the 3 nm-well LED (1.969 ps) is longer than that in the 4 nm-well LED (1.719 ps), it may be inferred that the dominant factor of modulation frequency is the carrier recombination lifetime τ_{r}, not the SCH delay time τ_{s}. τ_{r} is mainly decided by the carrier density N_{w} in the quantum well, therefore we can conclude that achieving higher modulation frequency is attributed to the higher carrier density.

6 Conclusion

We have investigated the circuit model of $In_{0.2}Ga_{0.8}N$/GaN single quantum well LEDs based on the rate equations. The time behavior of carriers in the SCH and well layer, carrier density and output power have been investigated. Then the static and dynamic behavior of both LEDs including *L-I* and modulation performance have been comparatively studied. In addition, our model can accurately demonstrate the effects of various well thickness on the static and dynamic characteristics.

Response Letter is available for this paper at:http://cjl.lightpublishing.cn/thesisDetails#10.37188/CJL.20250235

References:

[1] SINGH K J, HUANG Y M, AHMED T, *et al*. Micro-LED as a promising candidate for high-speed visible light communication [J]. *Appl. Sci.*, 2020, 10(20): 7384.

[2] TIAN P F, WU Z Y, LIU X Y, *et al*. Large-signal modulation characteristics of a GaN based micro-LED for Gbps

visible-light communication [J]. *Appl. Phys. Express*, 2018, 11(4): 044101.

[3] LIAO C L, CHANG Y F, HO C L, *et al*. High-speed GaN-based blue light-emitting diodes with gallium-doped ZnO current spreading layer [J]. *IEEE Electron Device Lett.*, 2013, 34(5): 611-613.

[4] SHI J W, CHI K L, WUN J M, *et al*. Ⅲ-nitride-based cyan light-emitting diodes with GHz bandwidth for high-speed visible light communication [J]. *IEEE Electron Device Lett.*, 2016, 37(7): 894-897.

[5] MCKENDRY J J D, GREEN R P, KELLY A E, *et al*. High-speed visible light communications using individual pixels in a micro light-emitting diode array [J]. *IEEE Photonics Technol. Lett.*, 2010, 22(18): 1346-1348.

[6] RASHIDI A, MONAVARIAN M, ARAGON A, *et al*. Nonpolar *m*-plane InGaN/GaN micro-scale light-emitting diode with 1.5 GHz modulation bandwidth [J]. *IEEE Electron Device Lett.*, 2018, 39(4): 520-523.

[7] DINH D V, QUAN Z H, ROYCROFT B, *et al*. GHz bandwidth semipolar ($11\bar{2}2$) InGaN/GaN light-emitting diodes [J]. *Opt. Lett.*, 2016, 41(24): 5752-5755.

[8] CHEN G C, FAN G H. Effect of n-type barrier doping on steady and dynamic performance of InGaN light-emitting diodes [J]. *Optoelectron. Lett.*, 2014, 10(4): 250-252.

[9] 陈贵楚, 范广涵. 量子阱数变化对InGaN/GaN发光二极管瞬态响应的影响 [J]. 发光学报, 2013, 34(10): 1346-1350.
CHEN G C, FAN G H. Transient analysis of InGaN/GaN light-emitting diode with varied quantum well number [J]. *Chin. J. Lumin.*, 2013, 34(10): 1346-1350. (in English)

[10] LI Z H, ZHANG X R, HAO Z B, *et al*. Bandwidth analysis of high-speed InGaN micro-LEDs by an equivalent circuit model [J]. *IEEE Electron Device Lett.*, 2023, 44(5): 785-788.

[11] RASHIDI A, NAMI M, MONAVARIAN M, *et al*. Differential carrier lifetime and transport effects in electrically injected Ⅲ-nitride light-emitting diodes [J]. *J. Appl. Phys.*, 2017, 122(3): 035706.

[12] LAN H Y, TSENG I C, KAO H Y, *et al*. 752-MHz modulation bandwidth of high-speed blue micro light-emitting diodes [J]. *IEEE J. Quantum Electron.*, 2018, 54(5): 3300106.

[13] MILANI N M, MOHADESI V, ASGARI A. A novel theoretical model for broadband blue InGaN/GaN superluminescent light emitting diodes [J]. *J. Appl. Phys.*, 2015, 117(5): 054502.

[14] 查内基. 半导体注入型激光器(Ⅱ)与发光二极管 [M]. 杜宝勋, 译. 北京: 清华大学出版社, 1991.
TSANG W T. *Semiconductor Injected Lasers and Light Emitting Diodes* [M]. DU B X, trans. Beijing: Tsinghua University Press, 1991. (in Chinese)

[15] LYSAK V V, KAWAGUCHI H, SUKHOIVANOV I A, *et al*. Ultrafast gain dynamics in asymmetrical multiple quantum-well semiconductor optical amplifiers [J]. *IEEE J. Quantum Electron.*, 2005, 41(6): 797-807.

[16] TANSU N, MAWST L J. Current injection efficiency of InGaAsN quantum-well lasers [J]. *J. Appl. Phys.*, 2005, 97(5): 054502.

[17] TSAI C Y, TSAI C Y, LO Y H, *et al*. Carrier DC and AC capture and escape times in quantum-well lasers [J]. *IEEE Photonics Technol. Lett.*, 1995, 7(6): 599-601.

[18] KAN S C, VASSILOVSKI D, WU T C, *et al*. Quantum capture and escape in quantum-well lasers-implications on direct modulation bandwidth limitations [J]. *IEEE Photonics Technol. Lett.*, 1992, 4(5): 428-431.

[19] ALAHYARIZADEH G, AGHAJANI H, MAHMODI H, *et al*. Analytical and visual modeling of InGaN/GaN single quantum well laser based on rate equations [J]. *Opt. Laser Technol.*, 2012, 44(1): 12-20.

[20] 赵勇兵, 钱晨辰. 载流子复合机制对InGaN绿光LED的Droop效应和调制带宽的影响 [J]. 照明工程学报, 2021, 32(4): 69-74.
ZHAO Y B, QIAN C C. Effect of carrier recombination mechanism on efficiency droop and modulation bandwidth of InGaN green LED [J]. *China Illum. Eng. J.*, 2021, 32(4): 69-74. (in Chinese)

[21] SHI J W, HUANG H Y, SHEU J K, *et al*. The improvement in modulation speed of GaN-based green light-emitting diode (LED) by use of n-type barrier doping for plastic optical fiber (POF) communication [J]. *IEEE Photonics Technol. Lett.*, 2006, 18(15): 1636-1638.

[22] 杨杰, 朱邵歆, 闫建昌, 等. 载流子复合机制对InGaN多量子阱蓝光LED调制带宽的影响 [J]. 发光学报, 2018, 39(2): 202-207.

YANG J, ZHU S X, YAN J C, *et al*. Effect of carrier recombination mechanism on modulation bandwidth of InGaN multiple-quantum-wells blue light emitting diodes [J]. *Chin. J. Lumin.*, 2018, 39(2): 202-207. (in Chinese)

陈贵楚(1973-),男,湖南岳阳人,博士,副教授,2009年于华南师范大学获得博士学位,主要从事光电子器件模拟研究。

E-mail: gchenbox@163.com